Energy 173 (2019) 971–984

Contents lists available at ScienceDirect

Energy

journal homepage: www.elsevier.com/locate/energy

Flexible electricity dispatch for CSP plant using un-fired closed air Brayton cycle with particles based thermal energy storage system

F. Rovense [a, *], M.A. Reyes-Belmonte [b], J. González-Aguilar [b, **], M. Amelio [a], S. Bova [a], M. Romero [b]

[a] University of Calabria (UNICAL), Department of Mechanical, Energy and Management Engineering (DIMEG), Via P.Bucci, Cubo 44C, 87036, Arcavacata di Rende, Cosenza, Italy
[b] IMDEA Energy Institute, Avda. Ramón de la Sagra 3, 28935, Móstoles, Madrid, Spain

ARTICLE INFO

Article history:
Received 25 September 2018
Received in revised form
22 January 2019
Accepted 17 February 2019
Available online 20 February 2019

Keywords:
CSP
Power cycles
Brayton cycles
Particles storage
Thermodynamics optimization

ABSTRACT

This paper presents a novel power block concept for flexible electricity dispatch in a Concentrating Solar Power (CSP) plant. The power block is based on intercooled – unfired regenerative closed air Brayton cycle that is connected to a pressurized solar air receiver. The Closed Brayton cycle uses a mass flow regulation system centered on the pressure regulation (auxiliary compressor and bleed valve) in order to control the Turbine Inlet Temperature (TIT). Doing so, the system is able to modulate turbine electricity production according to variations in the solar resource and changes in power electric demand. It has been found that the proposed power block is able to fully cover the electricity demand curve for those days with high solar resource. In case of integrating particles-based high temperature Thermal Energy Storage (TES) system, the power block can extend its production till the next day following the electricity curve demand during summer period. During winter period, the power plant can extend its production for a few hours due to the lower solar resource and the higher electric curve demand load.

1. Introduction

Concentrating Solar Power (CSP) is one of the most promising technologies for dispatchable renewable electricity production. This is based on its capacity to store large quantities of thermal energy at affordable costs, on the possibility of integrating CSP with conventional thermal power plants, on the wide availability of the solar resource and in the progressive reduction of the costs of this technology. For all the above mentioned reasons, scientific community, public opinion and governments are paying more and more attention to this technology. Despite obvious environmental benefits and abundant solar resource, a further step forward is needed for CSP deployment mainly due to the limited range of operating temperatures which, in turn, limit thermal conversion efficiency and, for the same energy production, cause a more extensive occupation of the land by the solar field. This translates into still high costs for electricity production compared to other renewable competitors (such as photovoltaics and wind power). Despite recent improvements and technology cost reduction for CSP, there is still wide margin of improvement. One of CSP trends for competitiveness improvement is based on the utilization of highly efficient thermodynamic cycles (such as combined cycles) or the use of alternative heat transfer fluids able to operate at temperature higher than current state-of-the-art molten salts 565 °C such as air, particles, liquid metals, supercritical steam or supercritical CO_2 [1–5]. In particular, the use of air as heat transfer fluid for CSP shows many interesting benefits as for example no water is required which is scarce source in areas with high interest for solar thermal electricity (deserts and arid areas). In addition, very high temperatures can be easily achieved (above 1000 °C), highly efficient arrangements such as Combined Cycles can be used, which are exhibiting working efficiencies above 50% [6]. Furthermore, very large power density (compared to steam cycles) can be achieved which in turns means more compact devices and faster transient response. In addition, air is abundant, cheap and it can be used whether as heat transfer fluid or working fluid. Nevertheless, there are some drawbacks about the use of air as heat transfer fluid for CSP. Main ones are related to the low air heat capacity that makes difficult the design of air solar receivers and difficulties for

* Corresponding author.
** Corresponding author.
E-mail addresses: francesco.rovense@unical.it (F. Rovense), jose.gonzalez@imdea.org (J. González-Aguilar).

https://doi.org/10.1016/j.energy.2019.02.135

thermal energy storage (TES). Some alternatives have been proposed for TES systems coupled to air power cycles (Brayton cycle) [7] but their main difficulties are related to materials compatibility for high temperature and low energy density. In this paper it is proposed intermediate TES system using particles as storing medium. Several works are showing the advantages and capabilities of coupling this type of TES to different working fluids [8–10].

Introduction of TES systems for CSP plants becomes mandatory on current scenario with high penetration of non-dispatchable renewable energy sources. In addition, the development of a new kind of electric production and distribution management, called "smart grid", has changed the power generation concept [11]. In that frame it is required a new set of power plants able to adapt their working conditions in order to follow the electrical demand curve and at the same time not polluting by minimizing hybrid options using fuels. In order to achieve that, renewable energy sources with storage capability becomes mandatory [12]. Solar resource is the favorite alternative for this aim, and concentrating solar power (CSP) with thermal energy storage (TES) becomes the more adapting technology [13].

There is significant amount of previous works focusing on the steady-state optimization of hybrid gas turbines coupled to a solar tower. Le Roux et al. [14] optimized solar receiver and recuperator through total entropy generation minimization for a solar dish using recuperated microturbine in order to maximize turbine output power under different weather conditions. Jansen et al. [15] focused into the optimization of the regenerators from open solar Brayton cycle. In other works [16], multi-objective optimization is made on large scale hybrid solarized gas turbine under steady state conditions. Di Gaeta et al. [17] investigated about the integration of micro gas turbine as stabilizer of energy grid by consuming hydrogen produced from the excess of electricity from a PV plant. On the contrary, in the present work, authors investigate about the feasibility of a closed Brayton cycle which uses only concentrating solar thermal energy for electricity production following real grid electric load curve. In order to do so, plant operation mode involves particles-based TES and closed-loop pressurized Brayton cycle. This novel power block concept allows electricity flexible dispatch and has not been applied yet to CSP. This results in a low environmental impact and a higher plant efficiency compared to state-of-the-art steam based CSP.

The work introduces significant novelty in the research on CSP plants:

- Annual production analysis of innovative closed-loop solarized Brayton cycle
- Solar plant design based on electricity demand curve
- Definition of the operational strategy that simultaneously adjusts the heliostats defocusing, the TES loading and unloading conditions and the closed-loop operation, to meet fluctuating electricity demand in real time

On the first part of this paper it is addressed the design of different CSP plant components. On the second part of the paper, different control strategies and system flexibility will be discussed. On the last section of the paper, CSP plant concept will be evaluated for Madrid (Spain) location using real data of small electric grid. Results analysis from daily, monthly and annual performance demonstrates the feasibility of this concept to fully cover electric demand of a small grid.

2. Plant description

2.1. Layout description

Plant general layout can be found in Fig. 1. As it can be observed, the plant is formed by two compressor stages (with intercooling in between), single stage turbine, solar tower, low temperature heat exchanger (for heat rejection) with cooling tower, particle heat exchanger, two storage tanks (of particles), mixing and splitting valves, auxiliary compressor and bleed valve for closed loop pressure regulation. In Fig. 1, the red line represents the air (HTF) path while the blue one refers to the water. The air flow enters in the compressor 1 and before entering the compressor 2, it is cooled in the intercooler. After leaving the compressor 2, the air is preheated by passing through the recuperator and then sent to the solar receiver where it is heated to the maximum possible temperature, limited by the properties of the materials and the available solar radiation. Part of the thermal energy of the air exiting the turbine (GT) can be recovered in the recuperator and used for air preheating

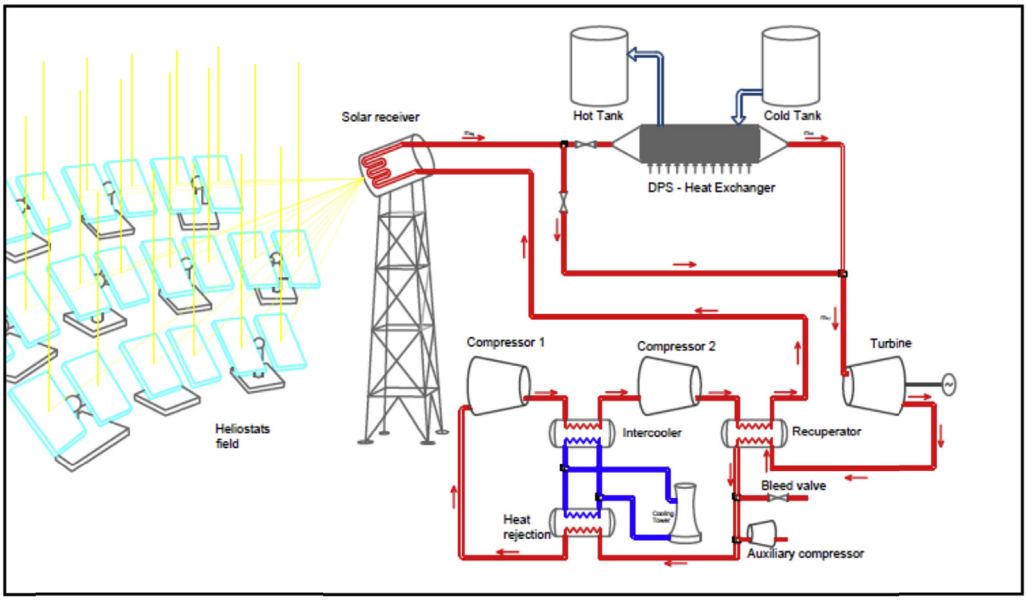

Fig. 1. General plant layout (during TES charging process).

upstream the solar receiver. Remaining heat from low-pressure stream will be rejected using heat rejection exchanger in order to cool down the air at a base temperature of 35 °C. Table 1 summarizes the main parameters of the power block.

The use of the gas turbine engine connected to the electric grid allows to rapidly follow the load or demand curve [18]. In addition, using a solar tower system is required as high concentrations and high temperatures are needed in order to increase the overall efficiency of the gas turbine power block in a pure solar system. It is clear that for enhancing solar share, it is necessary the use of thermal energy storage. This in turn would decrease the cost of electricity and CO_2 emissions due to its capability for electricity production at high demand peaks and fuel savings.

2.2. Un-fired closed Brayton power cycle

In past years, several projects have demonstrated the feasibility of solarized hybrid Brayton cycles [19–22]. Currently, unfired Brayton cycles research activities are mainly focused into the use of supercritical CO_2 cycles due to its high efficiency expectations for the moderate temperature level [23–26].

Regarding the use of air Brayton cycles for power generation, control mechanisms are required for adapting the working point of the turbine with changing heat input conditions from the solar plant and changes on the electricity curve demand. Basically, the system presented here uses a control strategy of the Turbine Inlet temperature (TIT) based on changing the circulating mass flow rate by a base pressure. The possibility to act over mass flow variation in a solarized conventional gas turbine to control TIT by using Variable Guide Vanes (VGV) was explored by Kitzmiller et al. [27]. They concluded that their use causes a decrease on the engine efficiency. In past works [28,29], the authors described the performance of mass flow regulation system in the closed solarized Brayton cycle in order to control the TIT by keeping constant the plant efficiency. The variation of the mass flow rate is obtained through a base pressure variation (at first compressor inlet) and consequently the cycle is pressurized. It is easy to notice (through the equations of the transformations of the typical Joule-Brayton cycle) that the pressure of the working fluid, in all the other points of the power plant, changes in proportion to that variation. Therefore, the mass contained in the internal volume of each component varies with the same law, as well as the density of the working fluid, at each point of the cycle, according to equation (1) [18].

$$\Delta M_c = \Delta \rho_c V_c = \frac{\Delta p_c}{RT_c} V_c \tag{1}$$

Another important consequence is the conservation of the volumetric flow in each section of the system. This is because the velocities of the fluid in a section depend on the ratio between the pressure upstream and downstream of that section and that ratio is always the same. Not having modified any of the sections, since the geometry of the plant is fixed, the volumetric flow rate, which is the product of speed by area of passage, is fixed and equal to the design value.

The mass flow rate, on the contrary, is variable with the fluid density, therefore it changes proportionally to the pressure, p_1.

In addition, it is observed that the correct mass flow air rate, G_C, defined by equation (2), remains unchanged, since the actual mass flow rate, G_1 varies proportionally to the pressure p_1, then the ratio $G_1/p1$ is constant. This is essential for the performance of the machines that depend precisely on the correct mass flow air rate and, therefore, remains constant at nominal operation for any mass flow rate:

$$G_c = \frac{G_1 \sqrt{RT_1}}{p_1} \tag{2}$$

Base pressure of the cycle is changed, according to need, by using the auxiliary compressor to add mass into the plant or the bleed valve to pull out air. The base temperature of the cycle is, instead, kept constant (by using the low temperature heat exchanger).

Table 1
Design parameters of the gas turbine and heat exchanger.

Parameter	Value
Compressor ratio [–]	6
Compressors polytrophic efficiency [%]	91.5
Turbine Polytrophic efficiency [%]	93.5
Max inlet GT pressure [bar]	5
Min inlet GT pressure [bar]	1.013
Intercooler pressure losses [%]	3
Recuperator pressure losses [%]	3
Heat rejection pressure losses [%]	3

2.3. Particles-based thermal energy storage system

Active thermal energy storage systems (TES) based on particles overcome some of the difficulties found on TES systems commonly used in commercial solar power plants, which use thermal oil or molten salts. On the one hand, particles-based active TES systems operate at wider temperature range than current commercial solutions [30,31]. In particular, particles can withstand temperature above 800 °C, which makes them suitable as TES solution for high temperature power cycles such as Brayton cycles [32]. On the other hand, particles do not show any limitation regarding minimum working temperature (as molten salts do), which reduces handling complexity of storing medium [33]. Furthermore, particles are inexpensive, can be easily transported and bulk stored in silos and are not hazardous. Nevertheless, main challenge about using particles as TES medium is related to the complex phenomena of heat exchange between the working fluid of the power cycle (in this case air) and the storing medium (particles). In order to allow for efficient heat exchange process between particles and working fluid (air), particles heat exchanger (FB-HX) design is based on fluidized-bed particles technology. In this case, particles will be fluidized using an air stream injected from the bottom of the FB-HX container, whilst pressurized air of the power cycle (Brayton cycle) will circulate inside horizontal tubes of the FB-HX [26,27] as it can be observed from Fig. 2.

Convection between dense particles suspension that is created around tubes is responsible for the heat transfer mechanism that can be estimated analytically [36]. As it was discussed on [10], there are several parameters that can be modified on FB-HX design such as number of stages, number of tubes, tubes diameters, distance between tubes, tubes length … Proper FB-HX design pursues assuring high efficiency of the heat exchanger, low pressure losses of the working fluid (pressurized air circulating inside FB-HX tubes) and small temperature difference between particles and working fluid, which will ensure that most of thermal energy will be transferred to the particles and later recovered. FB-HX tailored design for power cycle application can be found on Table 2.

Silicon carbide has been considered as the storing medium due to its excellent thermophysical properties that are shown in Table 3.

Temperature evolution of particles and working fluid (air) during discharging process can be found on Fig. 3. As it is observed, particles evolution is from 840 °C to 702 °C while discharging particles hot tank. At nominal design conditions, particles mass flow is 321 kg/s whilst the working fluid (pressurized air) is

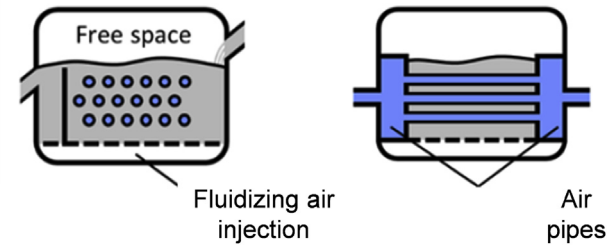

Fig. 2. FB-HX scheme.

increasing its temperature from 425 °C up to 835 °C and design mass flow of 94 kg/s which can ensure 800 °C for TIT. FB-HX has been designed for 30 bar pressurized air and pressure losses resulting into 0.33 bar.

As it was stated before, one of the main advantages about particles-based TES systems is related to the ease of storing and high temperature compatibility. Regarding storage, there is wide commercial experience on concrete silos for storing sand or hot particles (such as ashes). For hot particles storing concrete silos must be insulated internally to keep concrete temperatures below 200 °C [8]. In addition, concrete walls must be reinforced with post-tension strands on the periphery to improve concrete tension strength. For concrete silos sizing, it has been assumed cone bottom silo with 3:1 height to diameter ratio for the most economical silo size and assuming 30% of void fraction inside silos [8].

3. Control strategy and operation mode

The control strategy is defined in order to keep constant receiver outlet temperature at around 850 °C. This temperature is found suitable from previous research [37]. Air outlet temperature from the solar receiver can be fully controlled by actuating on heliostats field (thermal power incident into the receiver) and by modifying air mass flow circulating through the closed Brayton cycle (by the auxiliary compressor and bleeding valve). Depending on electricity demand curve and solar radiation, receiver outlet temperature and TIT would differ from 850 °C, due to the storage system.

In case the electricity demand is lower than the nominal power of the plant, a fraction of the hot air mass flow will be diverted towards the particles heat exchanger (as it can be observed on Fig. 4-a). This hot air will be used for charging particles storage system by transferring air heat into particles that will be flowing from cold tank to hot tank. After releasing its heat to the particles, the lower temperature air will join the hot air stream that is directly coming from the solar receiver and TIT will decrease. TIT reduction is necessary to control the gas turbine and to follow power demand requirements.

In case of concurrent high solar resource and low electricity demand, it is expected that high percentage of air mass flow rate will flow through the storage system to store the energy surplus and, at the same time, to reduce TIT which will reduce electricity production (Fig. 4.b and c). If the electricity demand increases, higher percentage of mass flow will directly go to the turbine obtaining a higher TIT.

Table 3
Silicon carbide particles properties.

Property	Units	Value
Sauter mean diameter	[μm]	63.9
Density	[kg m^{-3}]	3210
Specific heat capacity (at 500 °C)	[J kg^{-1} K^{-1}]	1150
Thermal conductivity (at 500 °C)	[W m^{-1} K^{-1}]	109

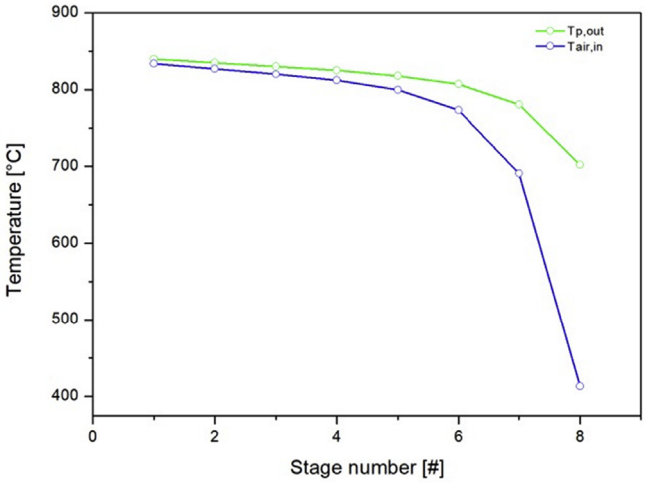

Fig. 3. Temperature evolution inside heat exchanger.

As it was mentioned above, the mass flow regulation is necessary in order to keep constant the air receiver outlet temperature. The auxiliary compressor and the bleed valve operate when there are irradiance variations; in particular, the auxiliary compressor introduces new mass of air when the direct normal radiation increases. On the contrary, the bleed valve pulls out air during the decrease of the DNI.

Energy required during low DNI periods is supplied by discharging the hot particles stored in the hot tank that are flowing through the heat exchanger. The mass flow regulation system continues to follow the demand curve, but in this case, the mass flow rate passes through the TES heat exchanger path. This keeps constant the outlet air temperature exiting the heat exchanger, therefore the TIT, at a constant value of 800 °C.

Solar power plant is based on pressurized closed air Brayton cycle and particles TES system, which introduces high degree of operation flexibility, as it is summarized on Table 4.

Different power plant actuators and layout arrangements are opening a wide range of possibilities for plant operation scenarios; some of the most interesting ones are listed below.

Table 2
Design parameters of the FB-HX.

Parameter	Value	Parameter	Value
Number of tubes per row	52	Total contact area of the tubes (m^2)	2042.2
Number of bundles	3	Total number of tubes	156
Number of rows	3	Active surface area of the tubes (m^2)	536
Tubes length (m)	23	Total length of the tubes (m)	3611
Particles mass flow (kg/s)	321.0	Total height of the heat exchanger (m)	1.4
Fluidization air mass flow (kg/s)	94.0	Air mass flow for the Brayton cycle (kg/s)	1.808

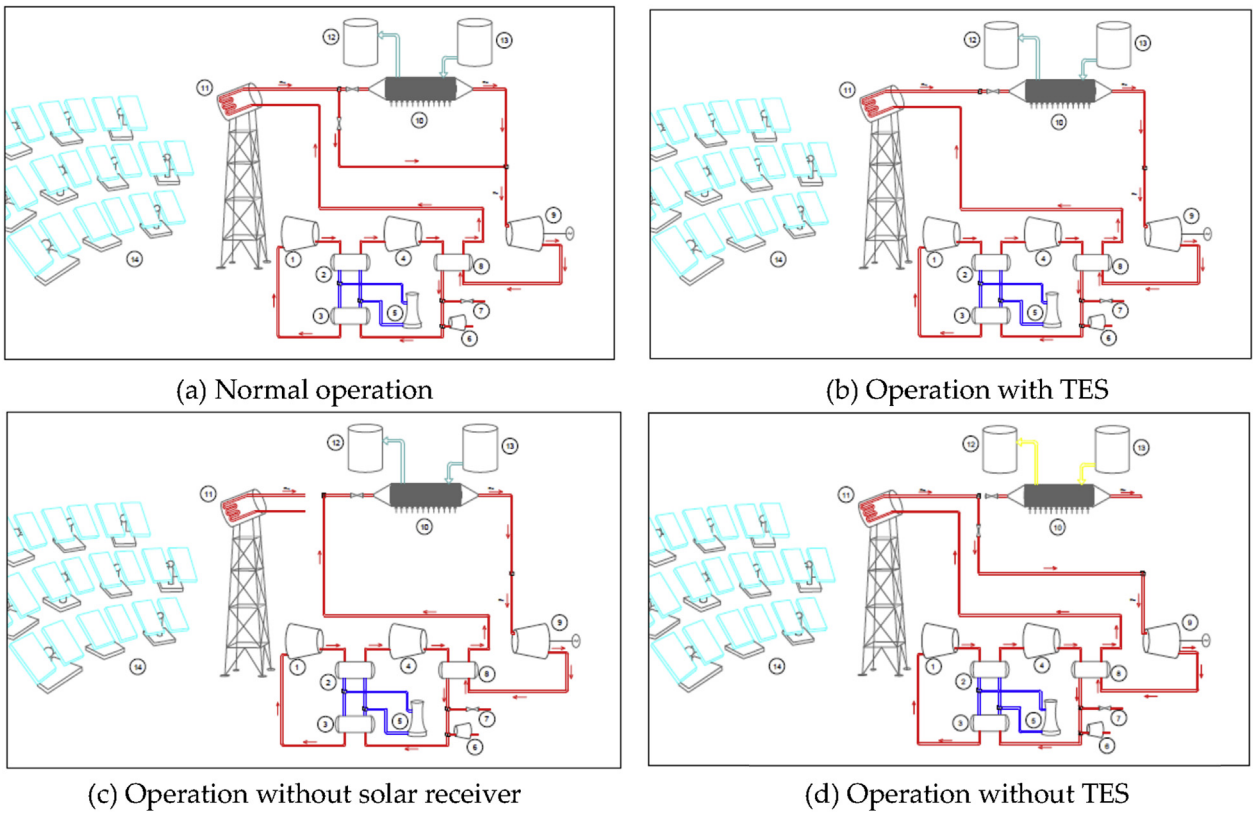

Fig. 4. Solar power plant arrangements: 1. Compressor 1; 2. Intercooler; 3. Heat rejection; 4. Compressor 2; 5. Cooling tower; 6. Auxiliary compressor; 7. Bleed valve; 8. Regenerator; 9. Turbine; 10. FB heat exchanger; 11. Solar receiver; 12. Hot particles silo; 13. Cold particles silo; and 14. Heliostat field. (a) Normal operation. (b) Operation with TES. (c) Operation without solar receiver. (d) Operation without TES.

Table 4
Operation modes.

Operation mode	Actuator	Controlled parameter	Adjusted parameter
Normal	Pressure regulation system (compressor and bleed valve)	Air receiver outlet temperature	Cycle air density
Normal	Heliostats defocusing system	Thermal power reaching the receiver	Average incident flux
Normal	Splitter tower two-way valve	Temperature inlet temperature	Air mass flow passing through with and without TES system path
TES discharge	Splitter Storage two-way valve	Temperature inlet temperature	Air mass flow passing through TES system path
Solar tower operation (without TES)	Pressure regulation system (compressor and bleed valve)	Air receiver outlet temperature/ Temperature inlet temperature	Air mass flow passing through without TES system path/air mass flow rate of the cycle
Solar tower operation (without TES) High DNI/no TES	Heliostats defocusing system	Air receiver outlet temperature/ Temperature inlet temperature	Air mass flow passing through without TES system path/air mass flow rate of the cycle
Solar tower operation (without TES) High DNI/no TES	Heliostats defocusing system	Air receiver outlet temperature	Air mass flow passing through without TES system path

- Solar plant aims to cover power demand curve during the day without storing any thermal energy (Fig. 4-**d**). In this case, turbine power production is controlled by means of pressure regulation (auxiliary compressor and bleed valve) and heliostats defocusing. In particular, the heliostats field control system performs in presence of high DNI in order to defocus a percentage of the heliostats; during these moments, the mass flow regulation system does not operate and the plant is totally pressurized at maximum allowed pressure. Vice–versa, the mass flow regulation system operates when there is lower solar radiation and all the heliostats are focused onto the receiver, as for example during sunrise and sunset [38]. In this case, the plant will only run when there is enough DNI available.
- Solar plant aims to cover power demand curve during the day and storing some thermal energy on particles. In this case, turbine will operate at lower TIT than in the previous one, due to air mixing, which will reduce the working efficiency. In this case, air mass flow passing through TES system (Fig. 4-**a**) will be regulated to follow demand curve. During periods of high DNI, the heliostats field control system performs in order to store the major energy and depending on the available TES volume. In this case, the air loop is pressurized and circulates the maximum mass flow rate inside the cycle. In case TES volume does not allows storing energy, heliostats field control system defocuses a percentage of heliostats in order to send onto the solar

receiver the needed thermal power. Mass flow regulation system regulates receiver outlet temperature.

- In case of low solar radiation and high electricity demand, solar field and TES actuates in order to follow the electrical load, as shown in Fig. 4-b. Thermal energy required from the GT is higher than the one that can be provided only from the solar field, and it is necessary TES discharging. In this case, all heliostats are focused and the power cycle is totally pressurized while all mass flow rate is passing through particles heat exchanger.
- In absence of solar radiation (during the night), the solar field does not operate and it is by-passed as shown in Fig. 4-c. Mass flow regulation operates in order to keep constant air outlet temperature of the heat exchanger following the demand curve (if possible). In this case, TES is discharged and through particles path only circulates the mass flow needed to transfer the thermal power required.
- Solar plant and power plant control strategy are designed for storing the highest amount of thermal energy into the particles during the day. In this case, air exiting FB-HX after exchanging its thermal energy with particles will be used for electricity production on the turbine. Its low temperature will be translated into lower efficiency of the turbine and lower power production. Thermal energy stored will be available for electricity production when desired as, for example, during night hours or for covering power peak demands.

4. Results and discussion

4.1. CSP sizing

Particles thermal storage is located between the solar tower and the turbine as it was shown in Fig. 1. Fluidized bed heat exchanger is needed to transfer heat from hot air to cold particles during charging process (excess of thermal power) and reverse from hot particles to medium temperature air when thermal power of the receiver is lower. Control strategy of particles based thermal energy storage system will depend on electricity demand curve and solar resource (DNI and sun position). Outlet air temperature from the heat exchanger has been chosen based on the percentage of the system peak power while FB-HX sizing was designed to ensure high temperature for particles storing. It is clear that the TIT and hence power plant production depends on the percentage of the mass flow rate flowing in each path.

The temperature at the outlet of the heat exchanger was chosen according to the electricity demand from actual data provided by smart-meters [39]. Fig. 5 shows the distribution of the demand curve with the percentage of the load factor for a representative residential demand curve. Maximum value (100%) was assumed equal to the peak power rate of the electric grid that is being analyzed (20 MW_e) which has the maximum value on January 15th. The design point of the solar field corresponds to the noon of the summer solstice (zenith angle, 14°) with a DNI of 850 W/m^2 (corresponding to 95 percentile of Madrid CDF).

Table 5 shows the results carried out by Thermoflex [40] to determine minimum air outlet temperature of the heat exchanger for its design. Column “hours” from Table 5 indicates the number of hours in which the power demand curve is lower than the corresponding percentage of the peak power. Air exit temperature from the table represents the air temperature exiting the heat exchanger and finally, ΔT is the air temperature difference between the receiver outlet and heat exchanger exit. In order to evaluate the minimum producible power rate (shown in Table 5), it was assumed that the total air mass flow rate flows through the heat exchanger path. On the contrary, the power rate of 20 MW_e is obtained when the total mass flow rate flows through the other path (straight to the turbine). As an example, 25% of plant peak power corresponds to 5 MW_e; in this case, electricity demand curve is lower than 5 MW_e for 271 h.

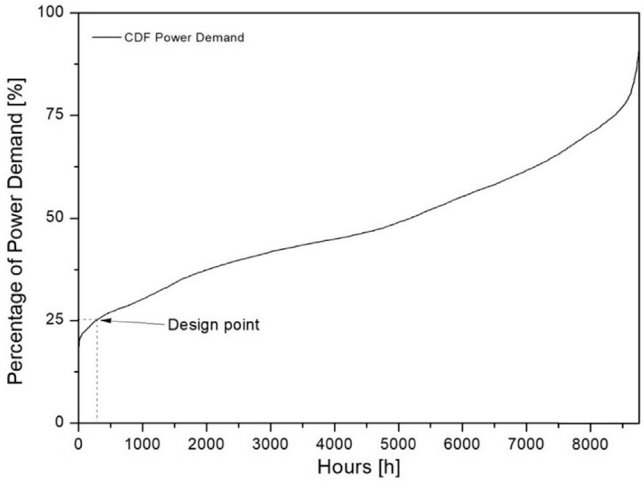

Fig. 5. Cumulative Distribution function of Curve Demand.

The most consistent cost item in the CSP system is represented by the solar field [41]. Therefore, solar multiple (SM) and the number of heliostats have the major impact. Optimum SM used for commercial CSP plants with thermal energy storage is in the range of 1.5–2.5 based on economic reasons [42]. In previous works, where molten salts were considered as the storing medium for considered unfired Brayton power cycle, optimum value of SM = 2 was found [43]. In the present work, two solar plants with SM 1.5 and SM 2 have been compared and the main data summarized in Table 6. Solar fields have been designed using WinDelsol [44], data from Table 6 and its corresponding optical matrix have been provided to Thermoflex for the yearly simulation. Temporary step of 1 h of data and TMY3 of Madrid for the calculations have been considered and therefore no big variations are expected for solar radiation along the day [45].

4.2. Daily performance

Daily analysis for three representative days of the year are discussed below to demonstrate the capability of the system to follow the electrical load of the demand curve and storing at the same

Table 5
Demand curve hours corresponding to the peak power percentage, air exit temperature and heat exchanger ΔT.

Hours [h]	Percentage of peak power	Corresponding power rate [MW]	HX Air exit temperature [°C]	Heat exchanger ΔT air path
1	15%	3	366.8	483.2
14	20%	4	395.2	454.8
271	25%	5	423.6	426.4
962	30%	6	451.9	398.1
1593	35%	7	480.2	369.8
2561	40%	8	500.0	350.0

Table 6
Solar field main data.

Parameter	Value	
Solar Multiple	2	1.5
Tower height [m]	113.4	98.18
Ratio of min/max field outer radius [−]	0.65	
Field inner radius [m]	85.03	73.64
Field span angle [°]	90	
Number of heliostats [−]	1656	1242
Reflective area per heliostats [m^2]	120	
Receiver panel effective width [m]	17.2	14.9
Receiver panel height [m]	13.76	11.92
Receiver average heat flux [kW m^{-2}]	400	
Reference design day	Summer solstice	
Receiver pressure loss [%]	10	

time the energy surplus into particle-based TES.

Fig. 6 shows demand curve for the summer solstice (21st of June). As it can be observed, there are two peak hours periods, one in the morning (from 7 to 11 h) and another one more evident in the evening (17 h). Due to the fact that the energy harvesting from the solar field (DNI curve) and the electric curve demand are shifted, TES system becomes mandatory in order to cover the electricity demand with reasonable solar field size. As it can be observed from the figure, power block can fully cover electricity demand from 9 h to 17 h with SM = 1.5 and from 8 h to 18 h with SM = 2.0, without any TES for summer days. In order to extend electricity production beyond 17 h or 18 h (when DNI is too low for satisfying electricity demand curve), the introduction of TES system is vital.

Fig. 7 shows demand curve and prediction of power plant electricity production curves with and without TES system for solar plant size designed for SM = 1.5 and 2.0. As it can be observed, the power plant without thermal storage (green line) produces electricity when there is enough DNI available. In this case, TIT control system is able to modulate power production of the turbine in order to satisfy electricity demand curve during central hours of the day (from 9 h to 17 h). However, during sunrise (from 7 h to 8 h) and sunset (from 17 h to 21 h) gas turbine cannot satisfy demand curve even with TIT control strategy.

During these hours, there is not enough solar resource and gas turbine will produce power below electricity demand curve. In case of considering TES system (red line), it is possible to store thermal energy surplus during central hours of the day into hot particles. This thermal energy will be recovered and transferred back to the air before entering the turbine in order to extend power production

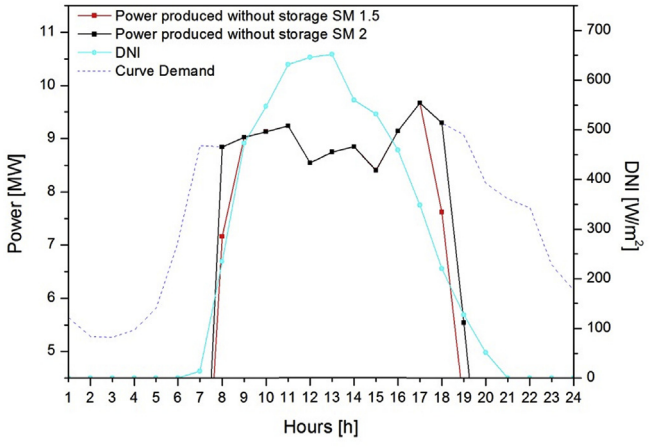

Fig. 6. Demand curve versus power production and DNI on June 21st.

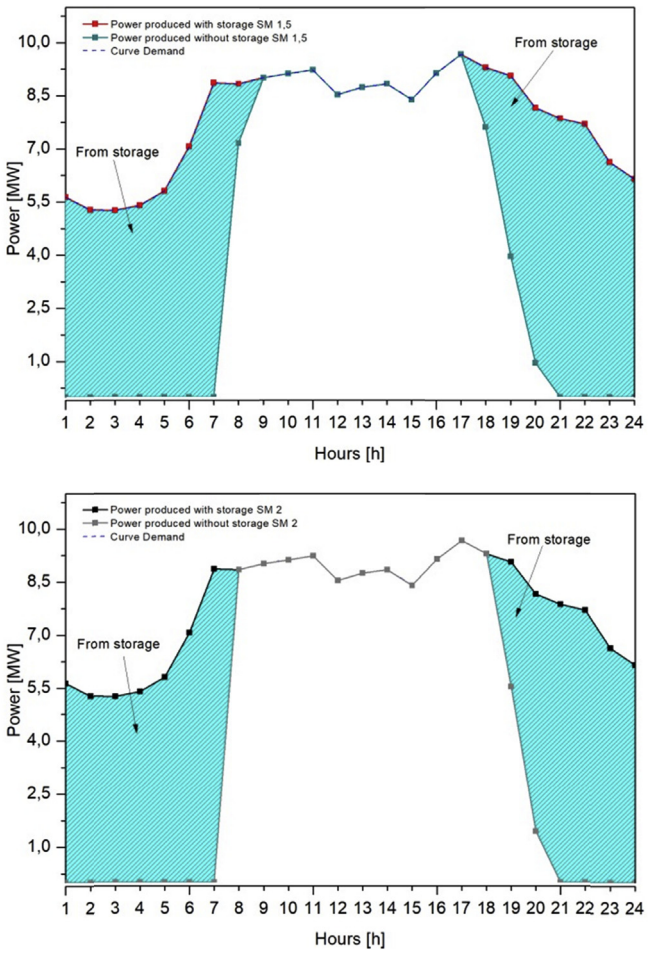

Fig. 7. Demand curve versus power production on June 21st of June. (Left) SM = 1.5; (right) SM = 2.0.

when DNI goes down. As it can be observed from red line, there was enough thermal energy stored during the day using SM = 1.5 configuration to extend the electricity production all along a summer day. In the case of SM = 2, it is possible harvesting extra thermal energy to be converted into electricity. Larger solar field also allows increasing power output produced at 19 h from 4 MW up to 5.5 MW. Logically, it is also possible to cover electricity power demand curve all along the day using TES for the case SM = 2.

When the peak power of the demand curve is lower than the rated power of the plant (20 MW_e), the surplus energy is stored by the particle thermal storage system as it is shown in Fig. 8. Effect of TES system operation can also be noted. The red line shows the case of the smaller solar power plant (SM = 1.5), while the black one shows the behavior of the larger system with SM = 2.0. As it can be noted, during non-zero DNI hours (from 8 h to 17 h) the amount of particles stored increases. During hours when DNI is decreasing (from 17 h to 20 h), the amount of particles stored at TES is decreasing in turns of satisfying electricity demand curve.

As it can be noted for 21st of June, in both simulated cases (SM = 1.5 and SM = 2.0) there are still enough particles stored once the sun is set (7 h–8 h). In other words, during summer time, particle tanks are not fully discharged for the chosen solar multiples and using the control strategy proposed. For the case of SM = 2.0, remaining particles inside storage tanks are triple than those for the case of SM = 1.5. This is translated into larger size of particles silos and the amount of bulk particles. It could be

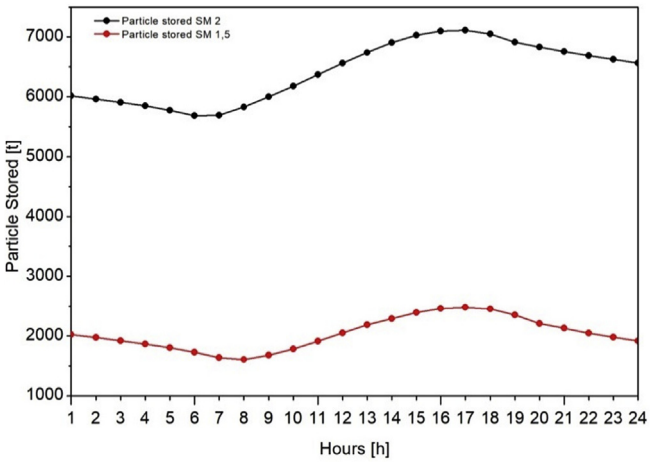

Fig. 8. Particle mass stored during 21st of June.

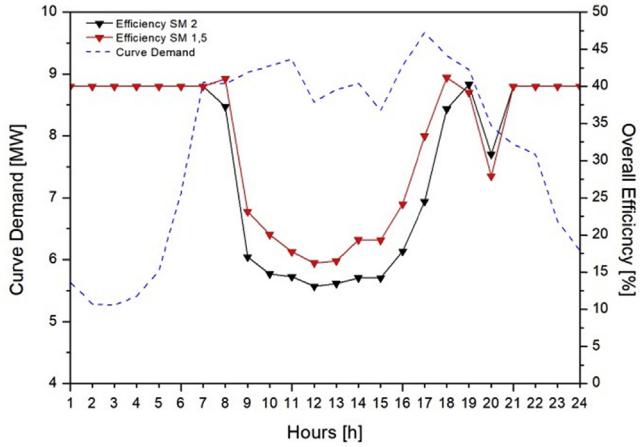

Fig. 9. Curve demand vs. power plant efficiency 21st June.

concluded that for summer days with high DNI, smaller solar plant (smaller SM) could be designed in order to satisfy electricity demand curve with no extra particles left inside tanks.

In case of high solar resource available, it could be desired a decrease on turbine power output in order to meet curve demand. To do so, increasing amount of air is diverted towards TES system which in turn will reduce TIT. It is clear that a reduction on TIT has an effect on plant net electric efficiency as it can be seen on Table 7 and also on Fig. 9. As it can be noted, power block efficiency decreases in occurrence of high solar radiation and low electric demand. In this case, the larger is the solar multiple of the plant the lower is the efficiency of the power block. As it can be deduced from Fig. 9 (at 20 h), when the TES is having an active role, the TIT is close to the temperature of hot particles stored (835 °C), the air mass flow rate has a peak value and the system performs at constant efficiency of 40%.

As it was observed on Fig. 7 (right), from 8 to 18 h (SM = 2.0) load demand could be satisfied with available DNI. This feature can be observed on Fig. 10 in terms of air mass flow repartition heading directly to the turbine and passing through TES. As it can be observed, mass flow rate passing through TES reaches its maximum during central hours of the day and transfers the surplus thermal energy to the storage particles. Despite the fact that receiver outlet temperature is kept constant at 835 °C, TIT decreases down to 500 °C during central hours of the day due to air mixing between stream passing through TES (below 400 °C) and the one heading directly to the turbine after leaving the receiver (835 °C). After the sun is set (20 h), there is no air heading directly to the turbine (due to low receiver outlet temperature) and air mass flow passes through TES in order to recover the stored heat which will result into TIT reaching 800 °C as it can be observed from Fig. 10.

In Fig. 11 it is shown the curve demand (dashed blue line) and the power produced by the two solar power plant designed SM = 1.5 (red line) and SM = 2.0 (black line) for the 21st of March. As it can be noted, operational hours of the plant are lower for 21st

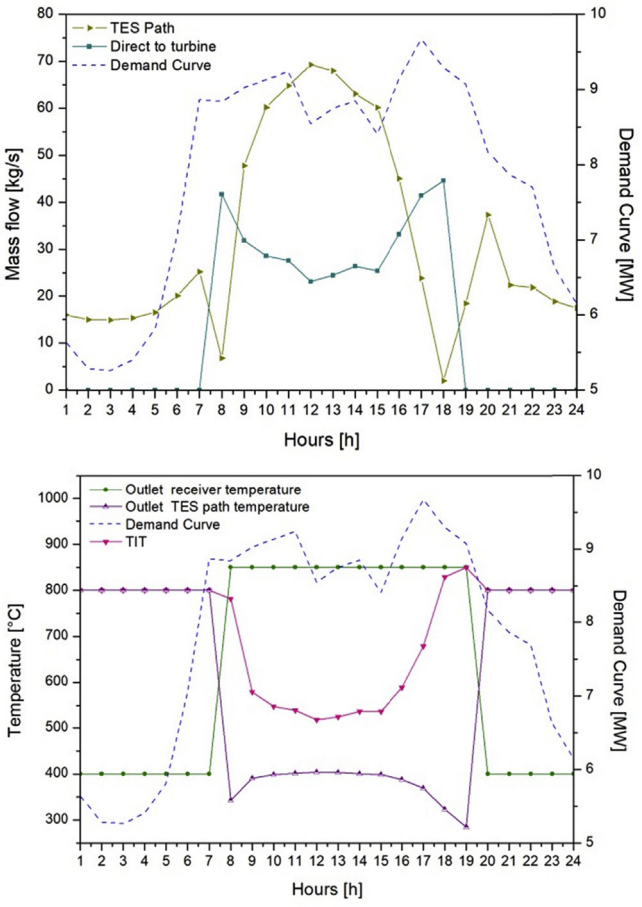

Fig. 10. Operation strategy for 21st June for SM = 2.0. (left) Air mass flow rate distribution. (right) Temperature control.

Table 7
Modelling results for different days.

	21st Dec		21st March		21st June	
SM	1.5	2	1.5	2	1.5	2
Number of hours for extended production	0	1	3	6	11	11
Total electricity produced (MWh)	77.48	103.33	188.98	215.44	187.82	187.82
Remaining particles stored by the end of the day (tons)	30.58	10.48	86.177	18.273	1917.79	6562.76
Averaged efficiency (%)	38.94	34.04	30.67	28.23	26.08	22.00

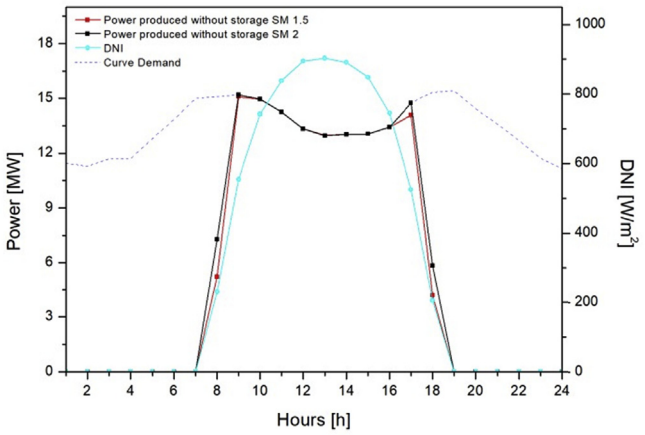

Fig. 11. Demand curve vs. power production 21st of March.

of March compared to 21st of June due to its lower DNI but also the higher electrical load demand. It can also be noted the change on the curve of the electrical power demand for spring time. Peak in the early morning moves to the left (it occurs from 7 h to 9 h) and the peak in the evening extend from 17 h to 19 h.

As it can be observed on Fig. 12, solar power plant without TES can satisfy electricity curve demand from 10 h to 16 h and it is close to the demand at 8 h and 17 h. However, electricity production significantly decreases by 18 h and by 19 h there is no power production of the solar plant designed for SM = 1.5. However, once TES system is included, the power block can extend power production till 21 h which is covering peak hour demand in the evening. Solar plant designed for SM = 2 is showing that without TES (grey line) the power block is able to satisfy electricity demand from 9 h to 17 h, while power produced at 8 h and 18 h is higher compared to the case from SM = 1.5. It can also be noted that considering TES system, power production can be extended till 23 h.

Fig. 13 shows the particle stored on 21st of March; as for the operational hours, the total mass of particles is lower with respect to the 21st of June. As it can be noted, hot tank is discharging in the evening and by the end of the day, storage tanks are technically discharged, although the stored mass is not zero. This is due to the fact that remaining particles stored are not enough to be transformed into electricity. It can also be noted that during high DNI hours there is enough thermal power gathered from the solar field for electricity production and for storing as hot particles. Once DNI decreases (between 16 and 17 h) storing tanks are discharging in order to provide the required heat for electricity production in the power block. As it can be noted, the higher the solar multiple the higher the amount of particles than can be stored. It can also be noted from Fig. 14 that the power block is operating at constant nominal efficiency during those hours when electricity demand is covered by discharging TES tanks (evening). As it was above-mentioned, whole air mass flow will pass through DPS heat

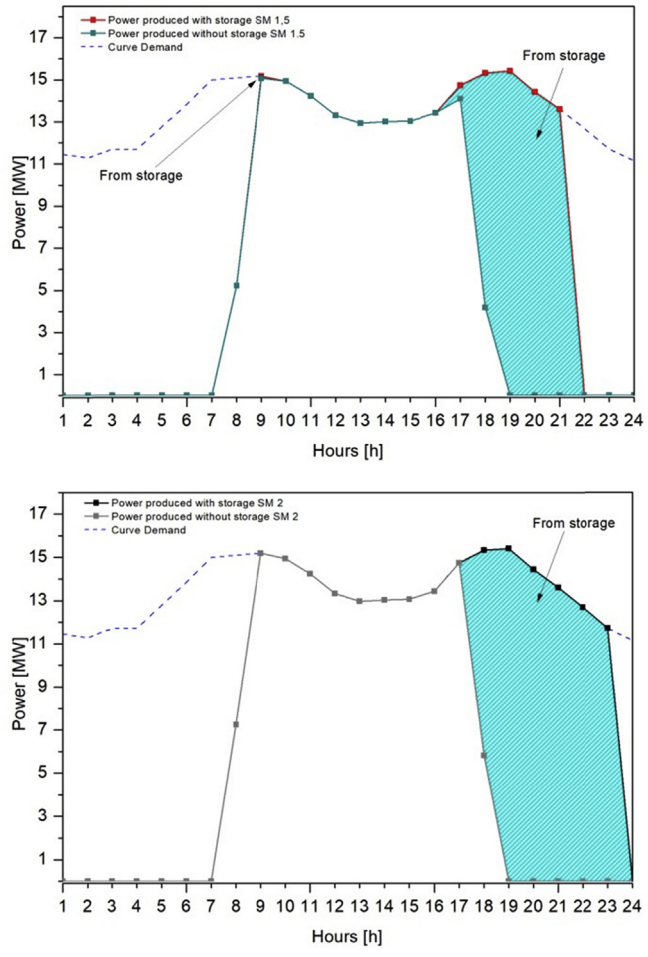

Fig. 12. Demand curve versus power production on March 21st. (Left) SM = 1.5, (right) SM = 2.0.

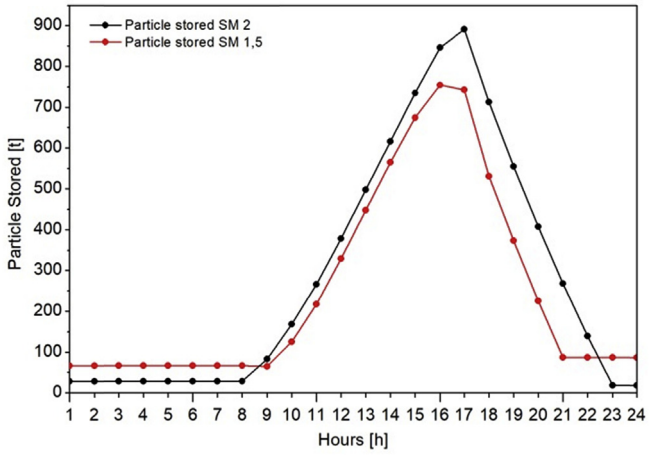

Fig. 13. Particle mass stored during 21st of March.

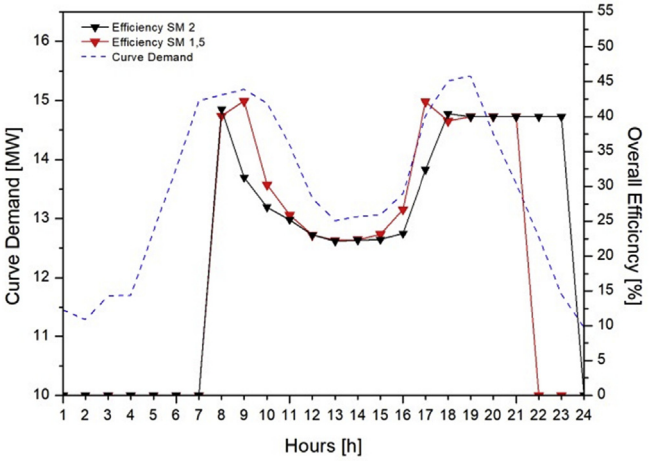

Fig. 14. Curve demand vs. power plant efficiency 21st March.

exchanger and achieve temperature close to 800 °C.

During winter season (for 21st December) due to the lower DNI and sunny hours and the high electricity demand (peak power is higher in winter than in summer or spring), the power plant reduces the number of working hours as it is shown in Fig. 15. Consequently, lower mass of particles can be stored. For the case of SM = 1.5 it can be observed from Fig. 16 that electricity production can be extended 1 h in the morning (11 h) and 1 h in the afternoon (15 h). It can also be noted that at 16 h there is not enough thermal energy for satisfying electricity curve demand due to the lower thermal energy harvested by the solar field (with low DNI conditions) but high power demand.

For the solar plant designed for SM = 2 power production at 10 h and 15 h can be satisfied without using thermal energy stored due to the larger power reaching the solar receiver and consequently to the power block. In the afternoon, electricity production can be satisfied at 16 h recovering heat from hot particles stored. In addition, remaining hot particles can supply electricity power demand at 20 h. Control strategy proposed for the solar plant assumes that the solar plant only produces electricity when there is enough power output to satisfy the demand curve. In case of lower net electrical power production than the demand curve, the turbine will not run as it can be observed in Fig. 16 (right) for 21st December for the case of SM = 2 (black line). Electricity production is stopped after 16 h but again producing at 20 h. There is a gap in production from 17 h to 20 h due to electricity demanded (blue dash line curve) is higher than it can be produced using stored particles. Furthermore, to allow following the demand curve, it is necessary to use the energy from the storage also in the middle hours of the day (13 h–15 h), as it can be noted in Fig. 17. As it can be noticed from Fig. 18, the power block operates at higher efficiency during winter time and for small solar plant design SM = 1.5. In that situation, power block is showing net efficiency above 35% for the whole day

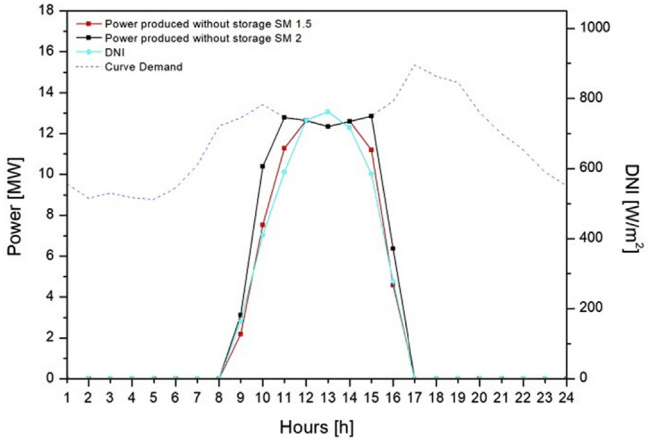

Fig. 15. Demand curve vs. power production and DNI 21st of December.

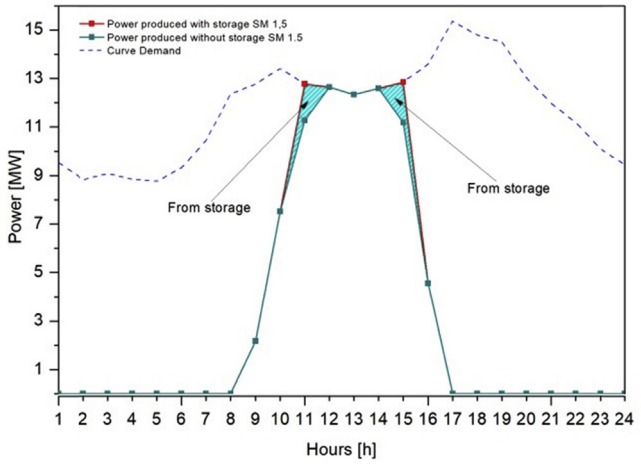

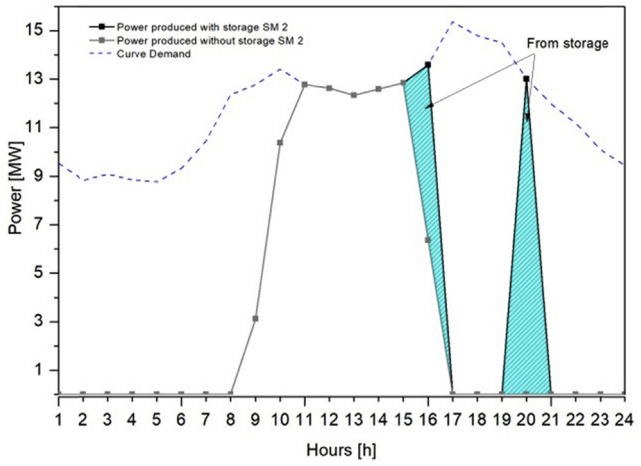

Fig. 16. Demand curve versus power production on December 21st. (Left) SM = 1.5; (Right) SM = 2.0.

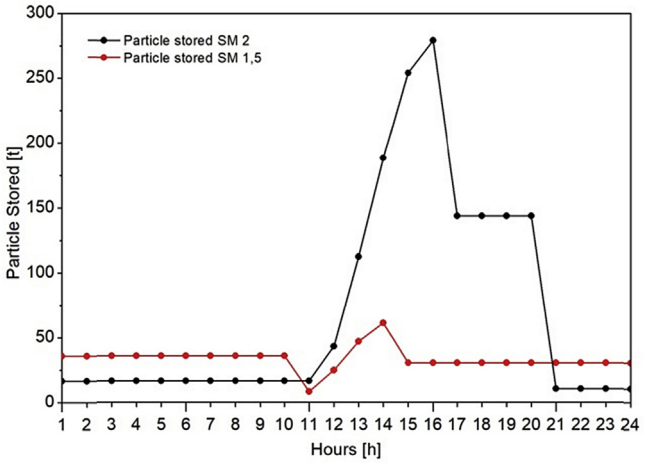

Fig. 17. Particle mass stored during 21st of December.

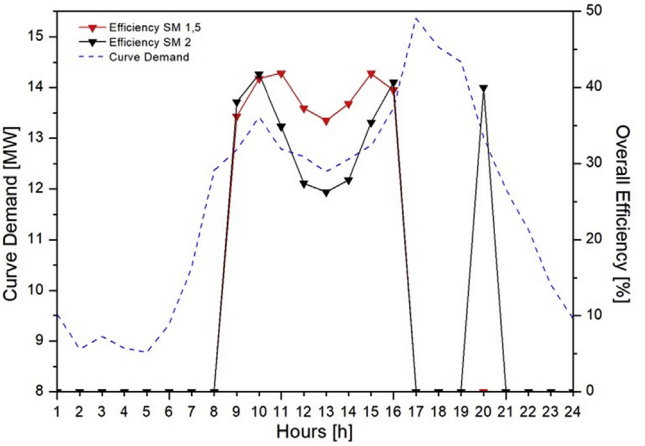

Fig. 18. Curve demand vs. power plant efficiency 21st December.

(21st December). This is based on the small amount of air that is diverted towards TES and later mixed with the air coming directly from solar receiver. This is due to the lower energy surplus that can be stored during winter time.

Table 8 shows TES tanks sizing for the three different days analyzed in detail in this section. Tanks sizing has been addressed considering maximum amount of particles that can be stored during each of the shown days. As it was shown on Figs. 7 and 8, for 21st of June there is enough surplus energy that TES can extend production overnight. For 21st of December, there is almost no

Table 8
TES tanks sizing.

Solar Multiple	1.5			2.0		
Day	21st December	21st March	21st June	21st December	21st March	21st June
Maximum amount of stored particles (ton)	60	750	2500	270	900	7000
Silo diameter (m)	3.4	6.4	10.7	5.2	6.7	13.7
Silo height (m)	10.1	18.9	29.0	13.7	19.8	39.0
Demand hours fully covered with TES (h)	0	3	12	1	5	12

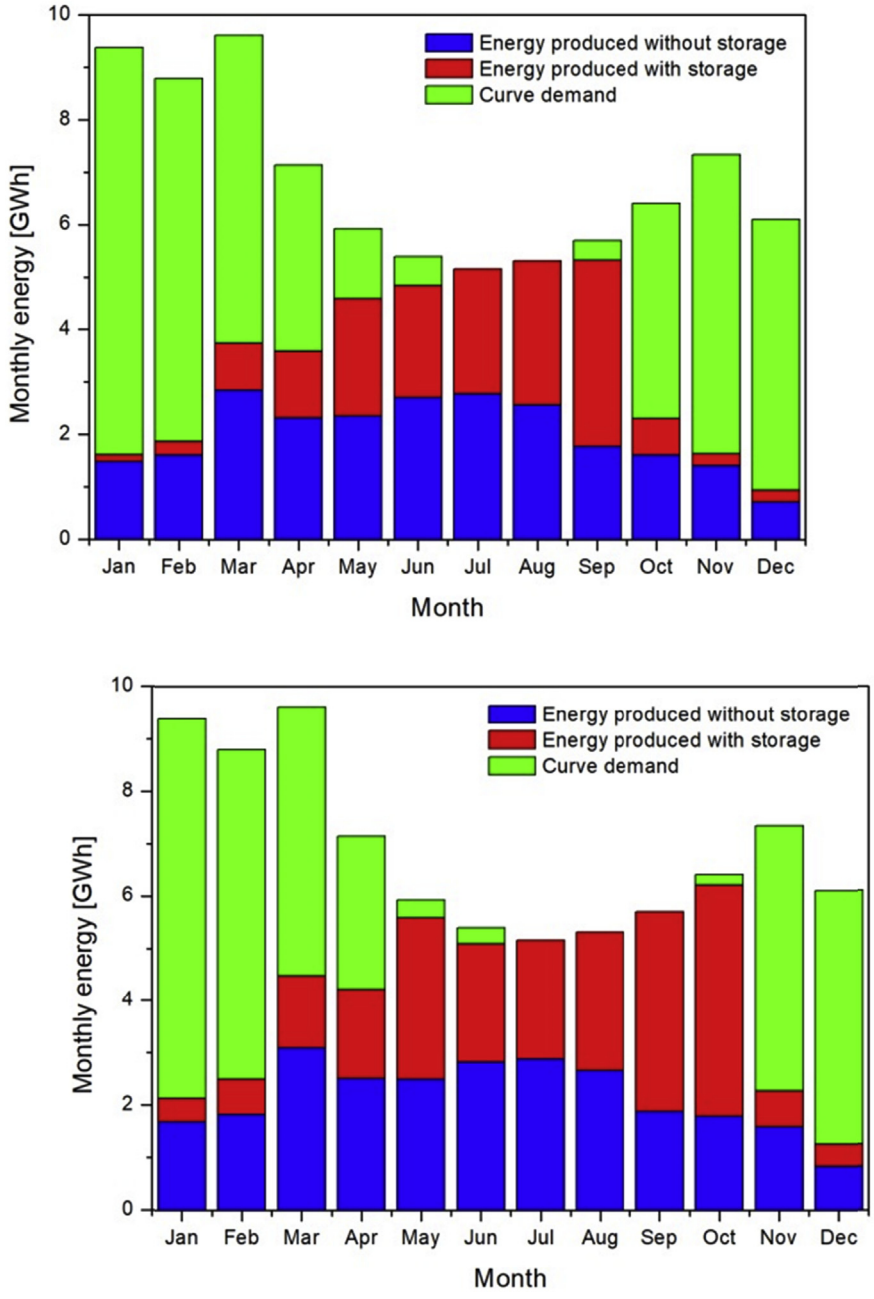

Fig. 19. Monthly energy. (Left) SM = 1.5; (right) SM = 2.0.

surplus energy to store (due to the higher electric demand and lower solar radiation) and particles tanks are relatively small.

4.3. Monthly performance

As it can be observed from Fig. 19 for SM = 1.5, power plant without TES is not able to fully satisfy monthly electricity curve demand (blue bars) as logical due to the plant cannot operate during night hours. As it can be noticed, the power plant when working together with TES system can fully satisfy electrical curve demand during summer months (July and August) based on the higher solar resource and the lower electricity demand. Even, there is a surplus of hot particles that are stored but are not needed for electricity production during summer months as it is shown on Fig. 20. On the contrary, from November to February, the solar resource is scarce but electricity demand is higher. During that time, the CSP plant contribution to satisfy electricity curve demand is very small due to the fact that CSP plant was sized for 21st June (when the solar resource was higher and the electric curve demand was lower). As it can be noticed from Fig. 19, the power plant designed for SM = 2 is able to extend electricity production and fully cover electricity demand during July, August and September. It can also be noticed that the power plant almost can cover whole electricity demand during May, June and October. For this size of plant (SM = 2), the amount of hot particles left inside the hot tank during the summer period is three times the case of SM = 1.5 (Fig. 20). The excess of thermal energy stored trims the power block efficiency between 2% and 4%, as it was observed in Table 7, due to the lower TIT. Nevertheless, the solar plant designed for SM = 2.0, with TES can extend its production and cover the electricity demand curve for a further 800 h, compared to the SM = 1.5 case. As it can be observed from Table 9, the proposed power plant concept without TES can meet the electricity demand around 3200 h per year, which represents 36% coverage. When particles-based TES is included, the power block can satisfy the electrical demand for 2000 extra hours; this increases coverage by up to 59% (SM = 1.5) and 68% (SM = 2.0).

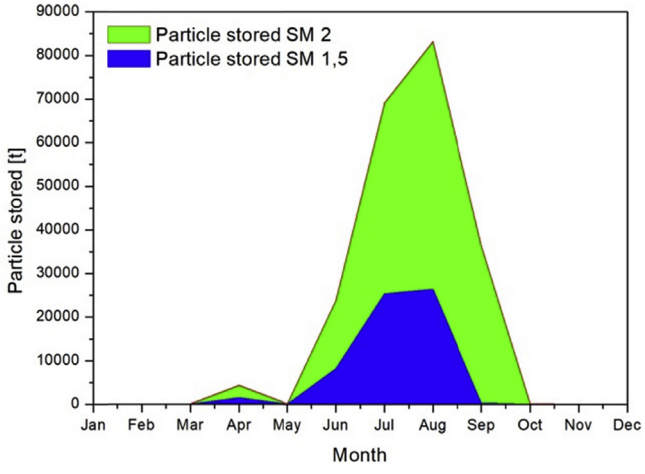

Fig. 20. Monthly Particle stored.

5. Conclusions

In this work, a novel concept of power block for CSP applications based on closed un-fired air Brayton cycle has been presented. The feasibility of the power block concept is coupled to an air receiver and solar field and it has been proved for electricity production from the energetic point of view. As it has been mentioned, the control strategy consists of varying receiver air outlet temperature and TIT by means of the mass flow rate regulation system. This concept of power plant is suitable to follow electricity demand curves during hours of high DNI without needing TES system. When particles-based TES system is introduced, the power plant can extend its production till the next day during summer periods. Indeed non-stop electricity generation has been obtained during July and August for SM = 1.5 and from July to September for SM = 2.0. In summary, the power plant is able to follow the electricity demand curve for a percentage ranging between 59% and 68% of the annual time, depending on solar multiple selection. Despite the annual increase in operating hours, achieved by changing SM = 1.5 to SM = 2.0 in the design of the plant, the largest solar field involved an excess of thermal energy available during the summer months. This led to a reduction of 2.5% power block efficiency, a triple amount of stored particles and only a slight improvement in the hours covered during summer time. As noted, benefits of larger solar field were only observed for the month of October.

It has been observed that TIT control system performs in very good way together with TES system in order to extend the power production after sunset, or to meet electricity demand curve during peak hours, when the solar resource is not enough. Particles-based TES system fits well as energy storage medium for the Brayton cycle due to its ability to work in a wide temperature range with neither minimum nor maximum temperature limitations.

Results presented into this work are proving the energetic feasibility of the power plant concept using only the solar resource. As it has been observed, the power plant can extend its production covering the electricity demand more than 2000 h when TES is included which represents up to 68% working hours of the year. As it was mentioned, power block concept is very flexible and electricity production can be rapidly controlled by modifying closed-loop pressure and TIT temperature. Proposed concept flexibility allows meeting variable electricity demand and also to get the most from available solar radiation which makes this concept suitable for smart-grids integration. In that case, generally, the distances between the generation plant and users are reduced and therefore, the absence of polluting emissions becomes even more important. Furthermore, the calculation of the annual energy yield provides an important parameter for assessing the feasibility of the installation, also from an economic point of view.

Table 9
Effect of Solar Multiple on annual plant performance (with storage).

SM	1.5	2
Total Energy produced by the power plant (with TES) [GWh]	40.91	49.89
Energy produced without TES [GWh]	24.38	26.36
Average Efficiency	28.67	26.17
Operational hours fully covering electricity curve demand (without TES)	3199	3252
Operational hours fully covering electricity curve demand (with TES)	5176	5979

CRediT authorship contribution statement

F. Rovense: Formal analysis, Writing - review & editing, Data curation, Conceptualization. **M.A. Reyes-Belmonte:** Formal analysis, Writing - review & editing, Writing - original draft. **J. González-Aguilar:** Writing - original draft, Supervision. **M. Amelio:** Writing - original draft, Writing - review & editing, Resources. **S. Bova:** Writing - review & editing, Supervision. **M. Romero:** Writing - original draft, Writing - review & editing, Project administration.

Acknowledgements

The research leading to these results has received funding from European Union's Horizon 2020 research and innovation program under grant agreement No 727762, Next-CSP project. Authors would also like to extend their gratitude to "Comunidad de Madrid" for its support to the ALCCONES project (S2013/MAE-2985) through the Program of R&D activities between research groups in Technologies 2103, co-financed by structural funds.

Nomenclature

CDF	Cumulative Distribution Function
CS	Concentrated Solar Power
DNI	Direct Normal Irradiation
DPS	Dense Particles Suspension
FB	Fluidized bed
GT	Gas Turbine
HX	Heat Exchanger
TES	Thermal Energy Storage
TIT	Turbine Inlet Temperature
GT	Gas Turbine
SM	Solar Multiple
ΔM_c	Air mass variation (added or bleed) in the cycle
$\Delta \rho_c$	Air density variation in the cycle
V_c	Volume of the cycle
ΔP_c	Base pressure variation
T_c	Average temperature
P_1	Instantaneous base pressure of the cycle
R	Ideal gas constant of air
T_1	Base temperature of the cycle

References

[1] Stein WH, Buck R. Advanced power cycles for concentrated solar power. Sol Energy 2017. https://doi.org/10.1016/j.solener.2017.04.054.
[2] Turchi CS, Ma Z, Neises TW, Wagner MJ. Thermodynamic study of advanced supercritical carbon dioxide power cycles for concentrating solar power systems. J Sol Energy Eng 2013;135:041007. https://doi.org/10.1115/1.4024030.
[3] Neises T, Turchi C. A comparison of supercritical carbon dioxide power cycle configurations with an emphasis on CSP applications. Energy Proc 2014;49:1187–96. https://doi.org/10.1016/j.egypro.2014.03.128.
[4] Blanco M, Santigosa LR. Advances in concentrating solar thermal research and technology. first ed. Woodhead Publishing; 2016.
[5] Reyes-Belmonte MA, Sebastián A, González-Aguilar J, Romero M. Performance comparison of different thermodynamic cycles for an innovative central receiver solar power plant. In: AIP conference proceedings. AIP Publishing LLC; 2017. p. 160024. https://doi.org/10.1063/1.4984558.
[6] Li Y, Yang Y. Thermodynamic analysis of a novel integrated solar combined cycle. Appl Energy 2014;122:133–42. https://doi.org/10.1016/J.APENERGY.2014.02.017.
[7] Kuravi S, Trahan J, Goswami DY, Rahman MM, Stefanakos EK. Thermal energy storage technologies and systems for concentrating solar power plants. Prog Energy Combust Sci 2013;39:285–319. https://doi.org/10.1016/j.pecs.2013.02.001.
[8] Ma Z, Zhang R, Sawaged F. Design of particle-based thermal energy storage for a concentrating solar power system. In: Proceedings of the ASME 2017 11th international conference on energy sustainability; 2017. p. 1–8.
[9] Ma Z, Mehos M, Glatzmaier G, Sakadjian B. Development of a concentrating solar power system using fluidized-bed technology for thermal energy conversion and solid particles for thermal energy storage. 2015. https://doi.org/10.1016/j.egypro.2015.03.136.
[10] Reyes-Belmonte MA, Díaz E, Romero M, González-Aguilar J. Particles-based thermal energy storage systems for concentrated solar power. AIP Conf Proc 2018;2033:210013. https://doi.org/10.1063/1.5067215.
[11] Momoh J. Smart grid fundamentals of design and analysis. John Wiley & Sons; 2012.
[12] Beaudin M, Zareipour H, Schellenberglabe A, Rosehart W. Energy storage for mitigating the variability of renewable electricity sources: an updated review. Energy Sustain Dev 2010;14:302–14. https://doi.org/10.1016/J.ESD.2010.09.007.
[13] Ellabban O, Abu-Rub H, Blaabjerg F. Renewable energy resources: current status, future prospects and their enabling technology. Renew Sustain Energy Rev 2014;39:748–64. https://doi.org/10.1016/J.RSER.2014.07.113.
[14] Le Roux WG, Bello-Ochende T, Meyer JP. Optimum performance of the small-scale open and direct solar thermal Brayton cycle at various environmental conditions and constraints. Energy 2012;46:42–50. https://doi.org/10.1016/j.energy.2012.03.034.
[15] Jansen E, Bello-Ochende T, Meyer JP. Integrated solar thermal Brayton cycles with either one or two regenerative heat exchangers for maximum power output. Energy 2015;86:737–48. https://doi.org/10.1016/j.energy.2015.04.080.
[16] Amiri F, Tahouni N, Azadi M, Panjeshahi MH. Design of a hybrid power plant integrated with a residential area. Energy 2016;115:746–55. https://doi.org/10.1016/j.energy.2016.09.038.
[17] di Gaeta A, Reale F, Chiariello F, Massoli P. A dynamic model of a 100 kW micro gas turbine fuelled with natural gas and hydrogen blends and its application in a hybrid energy grid. Energy 2017;129:299–320. https://doi.org/10.1016/j.energy.2017.03.173.
[18] Lozza G. Turbine a gas e cicli combinati. Esculapio; 2016.
[19] Heller P, Pfander M, Denk T, Tellez F, Valverde A, Fernandez J, Ring A. Test and evaluation of a solar powered gas turbine system. Sol Energy 2006;80:1225–30. https://doi.org/10.1016/j.solener.2005.04.020.
[20] Quero M, Korzynietz R, Ebert M, Jiménez AA, Del Río A, Brioso JA. Solugas - operation experience of the first solar hybrid gas turbine system at MW scale. In: Energy procedia; 2013. https://doi.org/10.1016/j.egypro.2014.03.193.
[21] Lanchi M, Montecchi M, Crescenzi T, Mele D, Miliozzi A, Russo V, Mazzei D, Misceo M, Falchetta M, Mancini R. Investigation into the coupling of micro gas turbines with CSP technology: OMSoP project. Energy Proc 2015;69:1317–26. https://doi.org/10.1016/J.EGYPRO.2015.03.146.
[22] Buck R, Giuliano S, Uhlig R. 16 – central tower systems using the Brayton cycle. In: Advances in concentrating solar thermal research and technology; 2017. p. 353–82. https://doi.org/10.1016/B978-0-08-100516-3.00016-2.
[23] Silva-Perez MA. Solar power towers using supercritical CO2 and supercritical steam cycles, and decoupled combined cycles. Elsevier Ltd; 2016. https://doi.org/10.1016/B978-0-08-100516-3.00017-4.
[24] Turchi CS. Project project summary Award: title: overall Budget: start date. 2013.
[25] Iverson BD, Conboy TM, Pasch JJ, Kruizenga AM. Supercritical CO2 Brayton cycles for solar-thermal energy. Appl Energy 2013;111:957–70. https://doi.org/10.1016/j.apenergy.2013.06.020.
[26] Reyes-Belmonte MA, Sebastián A, Romero M, González-Aguilar J. Optimization of a recompression supercritical carbon dioxide cycle for an innovative central receiver solar power plant. Energy 2016;112:17–27. https://doi.org/10.1016/j.energy.2016.06.013.
[27] Kitzmiller K, Miller F. Effect of variable Guide Vanes and natural gas hybridization for accommodating fluctuations in solar input to a gas turbine. J Sol Energy Eng 2012;134:041008. https://doi.org/10.1115/1.4006894.
[28] Rovense F, Perez MS, Amelio M, Ferraro V, Scornaienchi NM. Feasibility analysis of a solar field for a closed unfired Joule-Brayton cycle. Int J Heat Technol 2017;35:166–71. https://doi.org/10.18280/ijht.35Sp0123.
[29] Rovense F. A case of study of a concentrating solar power plant with unfired Joule-Brayton cycle. Energy Proc 2015;82:978–85. https://doi.org/10.1016/j.egypro.2015.11.855.
[30] Marti J, Haselbacher A, Steinfeld A. A numerical investigation of gas-particle suspensions as heat transfer media for high-temperature concentrated solar power. Int J Heat Mass Transf 2015;90:1056–70. https://doi.org/10.1016/j.ijheatmasstransfer.2015.07.033.
[31] Ho Clifford K. A review of high-temperature particle receivers for concentrating solar power. Appl Therm Eng 2016;109:958–69.
[32] Okoroigwe E, Madhlopa A. An integrated combined cycle system driven by a solar tower: a review. Renew Sustain Energy Rev 2016;57:337–50. https://doi.org/10.1016/j.rser.2015.12.092.
[33] Flamant G, Gauthier D, Benoit H, Sans J-L, Garcia R, Boissière B, Ansart R, Hemati M. Dense suspension of solid particles as a new heat transfer fluid for concentrated solar thermal plants: on-sun proof of concept. Chem Eng Sci 2013;102:567–76. https://doi.org/10.1016/j.ces.2013.08.051.
[36] Gomez-Garcia F, Gauthier D, Flamant G. Design and performance of a multi-stage fluidised bed heat exchanger for particle-receiver solar power plants with storage. Appl Energy 2017;190:510–23. https://doi.org/10.1016/j.apenergy.2016.12.140.
[37] Buck R, Bräuning T, Denk T, Pfänder M, Schwarzbözl P, Tellez F. Solar-hybrid gas turbine-based power tower systems (REFOS). J Sol Energy Eng 2002;124:2. https://doi.org/10.1115/1.1445444.
[38] Amelio M, Beraldi P, Ferraro V, Scornaienchi M, Rovense F. Optimization of heliostat field in a thermal solar power plant with an unfired closed Joule-

Brayton cycle. Energy Proc 2016;101:472–9. https://doi.org/10.1016/j.egypro.2016.11.060.
[39] SmartHG. Energy demand aware open services for smart grid intelligent automation. European Commision SmartHG project website; 2015. http://smarthg.di.uniroma1.it/ (accedido 25 de junio de 2018).
[40] Thermoflex. Thermoflex - Spotlight on solar thermal modeling. August 2012. , (s. f.).
[41] Kolb GJ, Ho CK, Mancini TR, Gary JA. Power tower technology roadmap and cost reduction plan. 2011.
[42] Jorgenson J, Denholm P, Mehos M, Turchi C. Estimating the performance and economic value of multiple concentrating solar power technologies in a production cost model. 2013.
[43] Rovense F, Amelio M, Ferraro V, Scornaienchi N. Analysis of a concentrating solar power tower operating with a closed Joule Brayton cycle and thermal storage. Int J Heat Technol 2016;34:485–90. https://doi.org/10.18280/ijht.340319.
[44] WinDelsol 1.0 users Guide. 2002.
[45] Sengupta M, Habte A, Kurtz S, Dobos A, Wilbert S, Lorenz E, Stoffel T, Renné D, Gueymard C, Myers D, Wilcox S, Blanc P, Perez R. Best practices handbook for the collection and use of solar resource data for solar energy applications. 2015.